CLASSIFICATION OF HYPERSPECTRAL DATA

B23APV01

PALLE PRANAY REDDY
Z RAM GOPAL
V GOWTHAM

MENTORED BY: Dr. ARUN PV

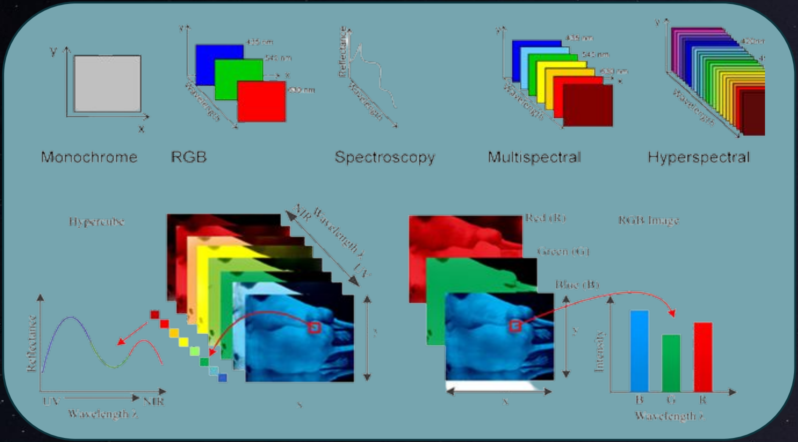

TABLE OF CONTENTS

01

INTRODUCTION

INTRODUCTION

What is HyperSpectral Data ?

- Unlike traditional RGB images, which only capture three bands of color (red, green, and blue), hyperspectral data can capture hundreds or even thousands of narrow and contiguous bands that cover a much wider range of the electromagnetic spectrum.

- Hyperspectral Imaging collects hundreds of channels at different wavelengths for the same spatial area.

- Each channel covers a certain range of wavelength of light reflected by the surface that is imaged.

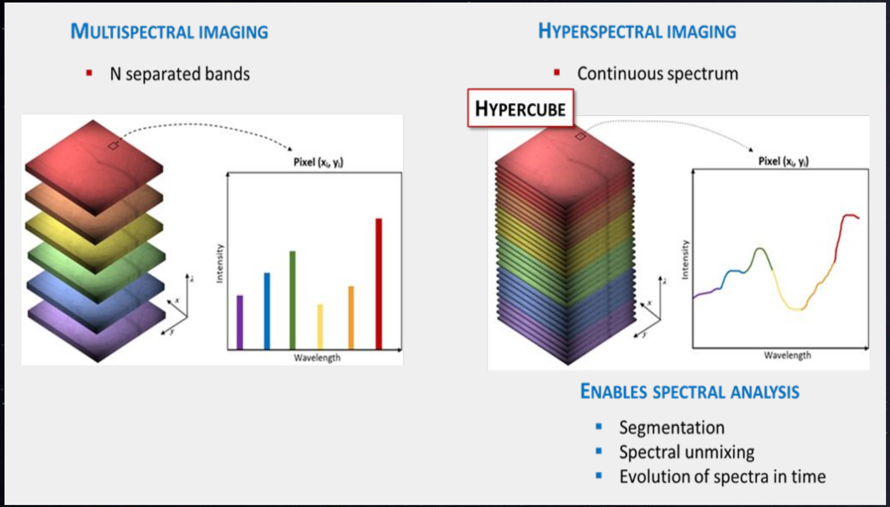

INTRODUCTION

HyperSpectral Data ?

- The collected data form a so-called hyperspectral cube, in which two dimensions represent the spatial extent of the scene and the third its spectral content.

- HSI has variety of applications, including remote sensing, environmental monitoring, mineral exploration, to map minerals in rocks and medical imaging in the field of computer vision

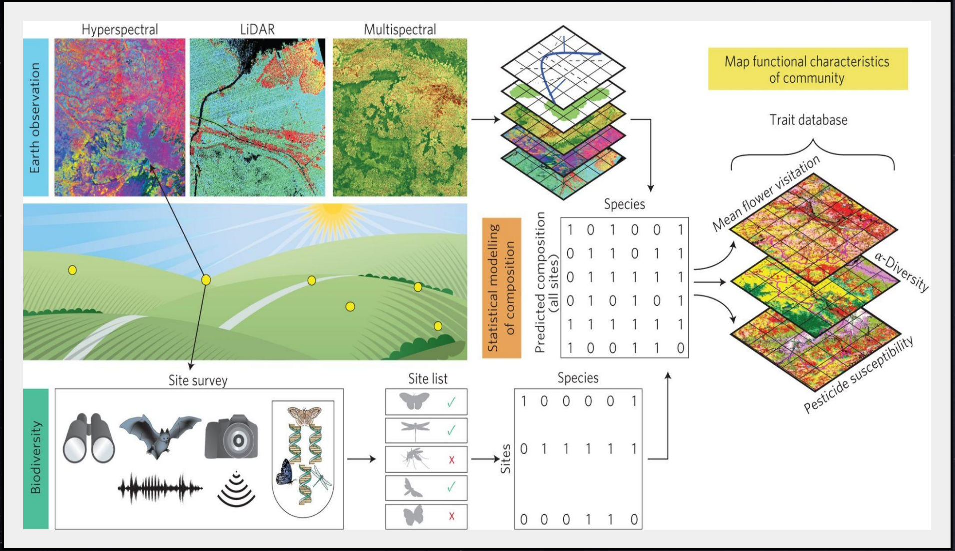

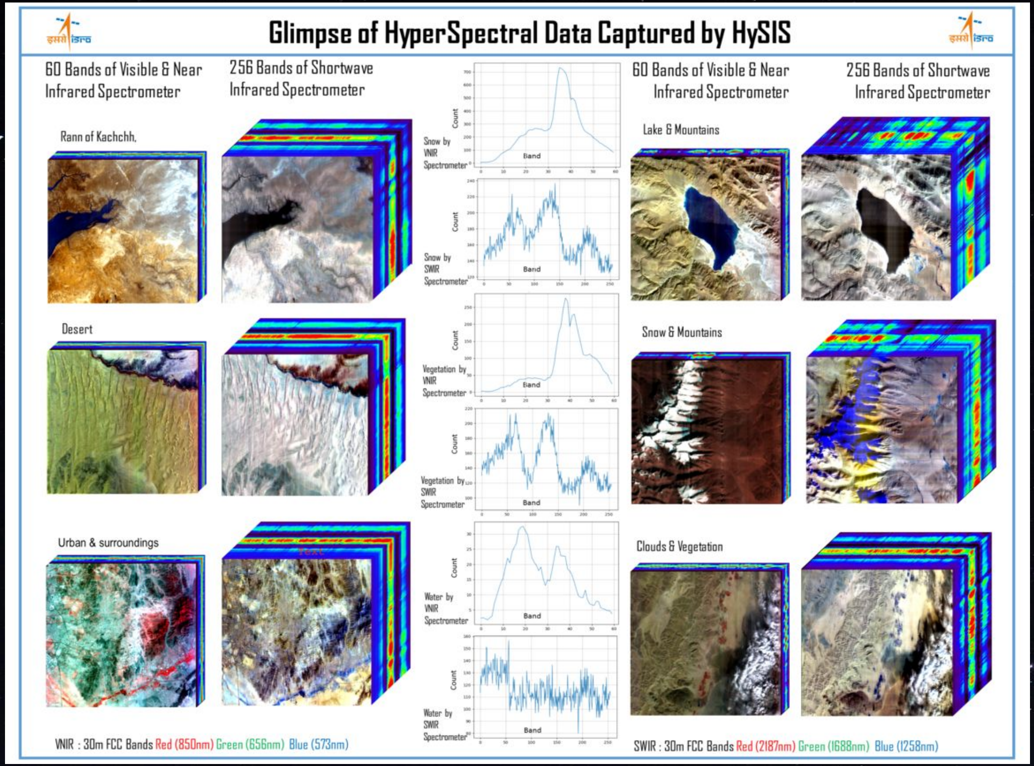

02

MOTIVATION

MOTIVATION

Why HyperSpectral Data ?

- Hyperspectral data provides a level of detail and accuracy that is not available with other types of remote sensing data. The ability to analyze materials in multiple bands across the electromagnetic spectrum allows for more precise identification of materials and objects.

- The detailed information captured in hyperspectral data can lead to new insights, such as identifying new mineral deposits.

- Hyperspectral imaging is employed in different fields such as astronomy, agriculture, molecular biology, biomedical imaging, mineralogy, geology, physics, cultural heritage, food processing, environment and surveillance

03

PROBLEM STATEMENT

PROBLEM STATEMENT

Mapping of Lunar Surface using Hyperspectral Image Classification

The hyperspectral data offers a platform for differentiating between minerals on the lunar surface, improving our comprehension of the composition of the moon's surface.

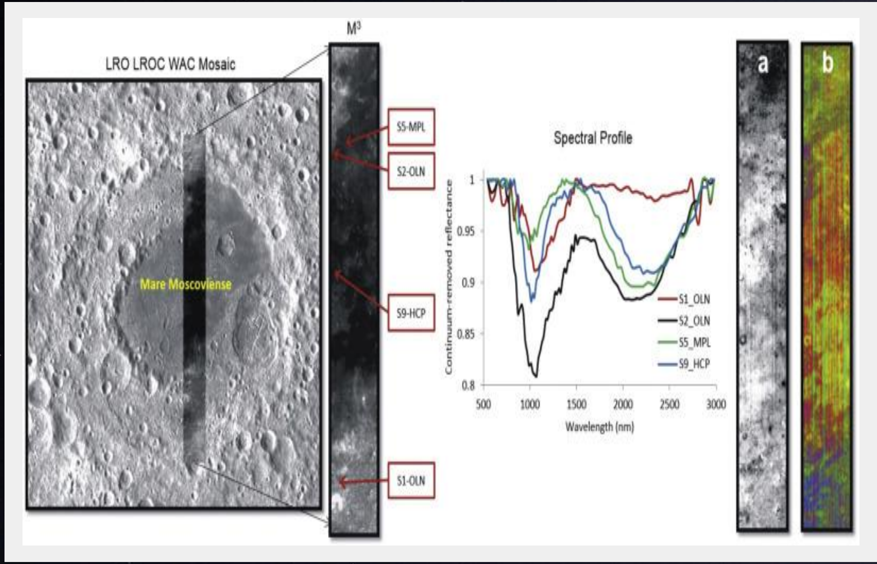

04

DATA INFORMATION

DATA INFORMATION

We are working on *Chandrayaan 2 IIRS data.*

Here's a brief information about IIRS:

Chandrayaan 2 Imaging Infrared Spectrometer (IIRS)

IIRS is designed to measure light from the lunar surface in narrow spectral channels (bands). It has the ability to split and disperse reflected sunlight (and its emitted component) into these spectral bands.

From the reflected solar spectrum, scientists will look for signatures, including of minerals. This will help map the lunar surface composition, which in turn will help us understand the Moon's origin and evolution in a geologic context.

DATA INFORMATION

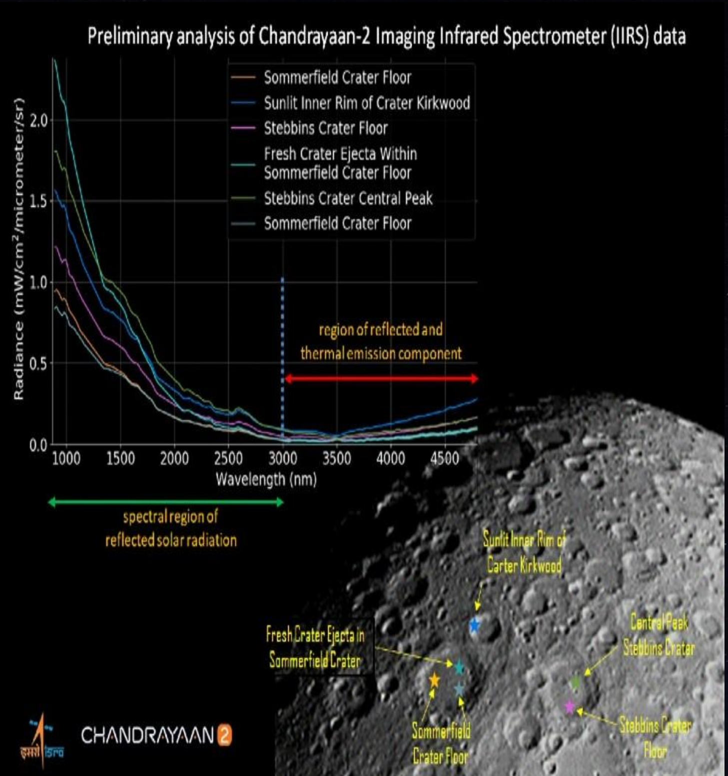

Information about the data:
Chandrayaan 2 IIRS Data

01 **Altitude - 100km**

02 **Spatial Resolution - 80m**

03 Spectral Resolution - 20 to 25 nm

04 Spectral Range - 0.8 to 5µm

05 **No. of Bands - Around 250**

05

ISSUES

ISSUES

Coarse spectral and spatial data

The smallest area resolved by the sensor is relatively large which means the details captured by the sensor are very less.

Noisy nature of data

Data is subjected to noise due to atmospheric effects of lunar surface and instrumental (sensor) noises.

Limited samples

Lack of enough samples cause model overfitting during training which significantly affects the model's performance.

Spatial and spectral context

Examining and labelling each pixel individually will not yield good results. The local spatio-spectral relationships of neighboring individual pixel vectors must also be studied.

06

LITERATURE SURVEY

LITERATURE SURVEY - I

Title: HybridSN: Exploring 3D-2D CNN Feature Hierarchy for Hyperspectral Image Classification

Author(s): Swalpa Kumar Roy, Student Member, IEEE, Gopal Krishna, Shiv Ram Dubey, Member, IEEE, and Bidyut B. Chaudhuri, Life Fellow, IEEE

Overview of HybridSN

- HybridSN is a study on hyperspectral image classification that explores the use of a hierarchical feature extraction approach combining 3D-CNN and 2D-CNN.
- The approach consists of two main components: a 3D-CNN that extracts spectral features from the hyperspectral data, and a 2D-CNN that extracts spatial features from the output of the 3D-CNN.
- The proposed HybridSN model achieved improved classification performance compared to existing models on several benchmark hyperspectral datasets.

LITERATURE SURVEY - I

Data Set(s)

- Indian Pines Dataset
- University of Pavia
- Salinas Scene Dataset

The flow diagram of HybridSN model

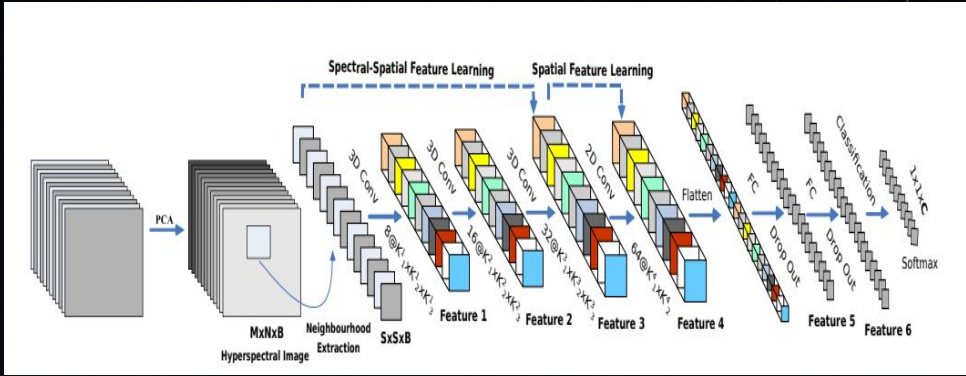

Result

TABLE III: The training time in minutes (m) and test time in seconds (s) over IP, UP, and SA datasets using 2D-CNN, 3D-CNN and $HybridSN$ architectures.

Data	2D CNN		3D CNN		HybridSN	
	Train(m)	Test(s)	Train(m)	Test(s)	Train(m)	Test(s)
IP	1.9	1.1	15.2	4.3	14.1	4.8
UP	1.8	1.3	58.0	10.6	20.3	6.6
SA	2.2	2.0	74	15.2	25.5	9.0

TABLE IV: The impact of spatial window size over the performance of $HybridSN$.

Window	IP(%)	UP(%)	SA(%)	Window	IP(%)	UP(%)	SA(%)
19×19	99.74	99.98	99.99	23×23	99.31	99.96	99.71
21×21	99.73	99.90	99.69	25×25	99.75	99.98	100

TABLE V: The classification accuracies (in percentages) using proposed and state-of-the-art methods on less amount of training data, i.e., 10% only.

Methods	Indian Pines			Univ. of Pavia			Salinas Scene		
	OA	Kappa	AA	OA	Kappa	AA	OA	Kappa	AA
2D-CNN	80.27	78.26	68.32	96.63	95.53	94.84	96.34	95.93	94.36
3D-CNN	82.62	79.25	76.51	96.34	94.90	97.03	85.00	83.20	89.63
M3D-CNN	81.39	81.20	75.22	95.95	93.40	97.52	94.20	93.61	96.66
SSRN	98.45	98.23	86.19	99.62	99.50	99.49	99.64	99.60	99.76
HybridSN	98.39	98.16	98.01	99.72	99.64	99.20	99.98	99.98	99.98

LITERATURE SURVEY - II

Title: Graph Convolutional Networks for Hyperspectral Image Classification

Author(s): Danfeng Hong , Member, IEEE, Lianru Gao , Senior Member, IEEE, Jing Yao , Bing Zhang , Fellow, IEEE, Antonio Plaza , Fellow, IEEE, and Jocelyn Chanussot , Fellow, IEEE

Overview of GCN in Feature Space for Image

- Graph Convolutional Networks (GCNs) capable of taking advantage of both spatial and spectral information. Hence they can be used for Hyperspectral Image Classification
- Since GCNs have drawbacks like high computational cost, allowance of only full-batch network learning etc., the authors proposed miniGCNs which follows mini-batch learning and overcomes the above mentioned drawbacks.
- The experimental results, conducted on three widely used HS data sets, demonstrate the effectiveness and superiority of the proposed miniGCNs compared to the traditional GCNs.

LITERATURE SURVEY - II

Data Set(s)

- Indian Pines
- Pavia University
- Houston2013

The flow diagram of GCN model

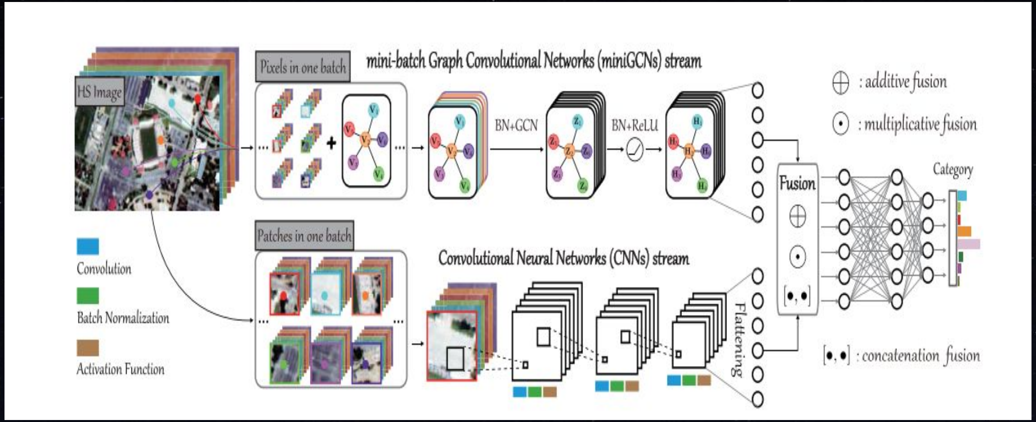

Result

TABLE V

QUANTITATIVE COMPARISON OF DIFFERENT ALGORITHMS IN TERMS OF OA, AA, AND κ ON THE INDIAN PINES DATA SET. THE BEST ONE IS SHOWN IN BOLD

Class No.	KNN	RF	SVM	1-D CNN	2-D CNN	3-D CNN	GCN	miniGCN	FuNet-A	FuNet-M	FuNet-C
1	45.45	57.80	67.34	47.83	65.90	66.26	65.97	**72.54**	68.64	69.51	68.50
2	46.94	56.51	67.86	42.35	76.66	71.94	72.70	55.99	80.99	**82.40**	79.59
3	77.72	80.98	93.48	60.87	92.39	97.28	87.50	92.93	95.11	94.57	**99.46**
4	84.56	85.68	94.63	89.49	93.96	95.08	93.74	92.62	**96.64**	96.42	95.08
5	80.06	79.34	88.52	92.40	87.23	88.09	91.39	94.98	95.41	**96.99**	95.70
6	97.49	95.44	94.76	97.04	97.27	98.18	97.49	98.63	99.32	**99.54**	**99.54**
7	64.81	**77.56**	73.86	59.69	77.23	75.38	75.38	64.71	72.98	76.80	75.93
8	48.68	58.85	52.07	65.38	57.03	56.29	51.70	68.78	**70.31**	58.97	68.90
9	44.33	62.23	72.70	**93.44**	72.87	78.01	62.77	69.33	74.82	74.82	71.63
10	96.30	95.06	98.77	99.38	**100.00**	**100.00**	96.91	98.77	99.38	99.38	99.38
11	74.28	88.75	86.17	84.00	**92.85**	90.59	86.25	87.78	85.93	79.50	89.55
12	15.45	54.24	71.82	86.06	88.18	90.30	66.97	50.00	**93.03**	91.21	91.52
13	91.11	97.78	95.56	91.11	**100.00**	**100.00**	95.56	**100.00**	**100.00**	**100.00**	**100.00**
14	33.33	56.41	82.05	84.62	84.62	74.36	71.79	48.72	79.49	82.05	**94.87**
15	81.82	81.82	90.91	**100.00**	**100.00**	**100.00**	81.82	72.73	**100.00**	**100.00**	**100.00**
16	40.00	**100.00**	**100.00**	80.00	**100.00**	**100.00**	**100.00**	80.00	**100.00**	**100.00**	**100.00**
OA (%)	59.17	69.80	72.36	70.43	75.89	75.48	71.97	75.11	79.76	76.76	**79.89**
AA (%)	63.90	76.78	83.16	79.60	86.64	86.36	81.12	78.03	88.25	87.64	**89.35**
κ	0.5395	0.6591	0.6888	0.6642	0.7281	0.7240	0.6852	0.7164	0.7698	0.7382	**0.7716**

TABLE VI

QUANTITATIVE PERFORMANCE COMPARISON OF DIFFERENT ALGORITHMS IN TERMS OF OA, AA, AND κ ON THE PAVIA UNIVERSITY DATA SET. THE BEST ONE IS SHOWN IN BOLD

Class No.	KNN	RF	SVM	1-D CNN	2-D CNN	3-D CNN	GCN	miniGCN	FuNet-A	FuNet-M	FuNet-C
1	73.86	79.81	74.22	88.90	80.98	80.69	76.49	96.35	**96.99**	96.47	96.67
2	64.31	54.90	52.79	58.81	81.70	89.12	70.15	89.43	**97.74**	97.36	97.60
3	55.10	46.34	65.45	73.11	67.99	65.90	62.70	**87.01**	83.98	83.44	84.49
4	94.95	**98.73**	97.42	82.07	97.36	98.45	98.35	94.26	96.45	84.40	89.95
5	99.19	99.01	99.46	99.46	99.64	99.19	99.37	99.82	99.55	**100.00**	99.64
6	65.16	75.94	93.48	**97.92**	97.59	92.37	83.22	43.12	71.33	85.30	90.56
7	84.30	78.70	87.87	88.07	82.47	76.04	88.38	**90.96**	66.67	63.80	78.27
8	84.10	90.22	89.39	88.14	**97.62**	95.81	92.33	77.42	69.61	71.53	71.73
9	98.36	97.99	**99.87**	**99.87**	95.60	95.72	95.72	87.27	99.86	99.22	98.04
OA (%)	70.53	69.67	70.82	75.50	86.05	88.44	77.99	79.79	89.00	90.34	**92.20**
AA (%)	79.68	80.18	84.44	86.26	88.99	88.14	85.19	85.07	86.91	86.84	**89.66**
κ	0.6268	0.6237	0.6423	0.6948	0.8187	0.8472	0.7196	0.7367	0.8540	0.8709	**0.8951**

LITERATURE SURVEY - III

Title: FPGA: Fast Patch-Free Global Learning Framework for Fully End-to-End Hyperspectral Image Classification

Author(s): Zhuo Zheng, Student Member, IEEE, Yanfei Zhong, Senior Member, IEEE, Ailong Ma, and Liangpei Zhang, Fellow, IEEE.

Summary of FPGA

- The FPGA architecture is composed of a **deep convolutional neural network (CNN)** that extracts spectral features from the hyperspectral data and a **global average pooling layer** that aggregates the spectral features into a single feature vector for each pixel.
- Several evaluation metrics are used to measure the accuracy of the model, including overall accuracy, kappa coefficient, and producer's and user's accuracy.
- The drawbacks of the FPGA framework include: the size of the FPGA model can be quite large, which can make it difficult to train and deploy on resource-limited devices; the FPGA model requires a large amount of training data to achieve high accuracy, which can be challenging to obtain for certain applications.

LITERATURE SURVEY - III

Data Set(s)

- ROSIS-03 Pavia University
- Salinas Dataset
- CASI University of Houston

The flow diagram of FPGA model

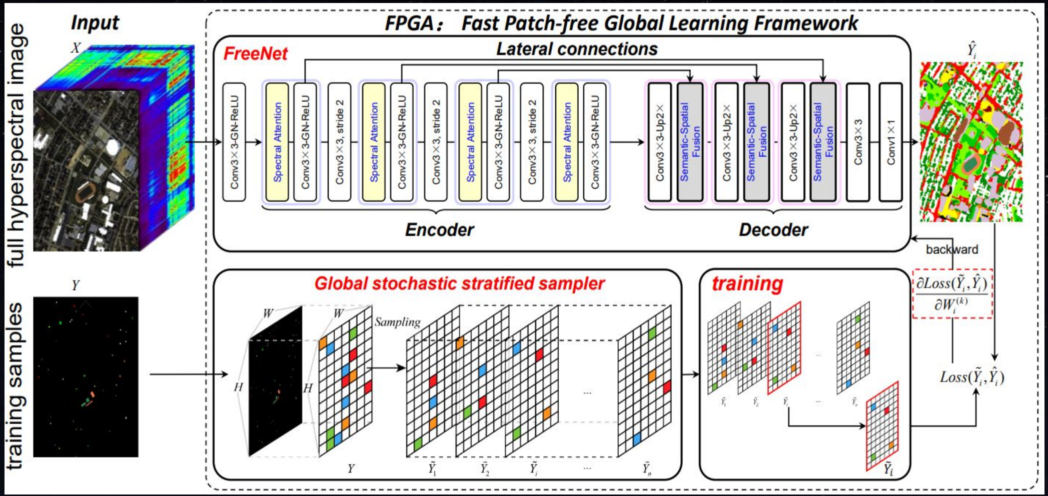

Result

TABLE II
THE NUMBER OF TRAINING SAMPLES AND TEST SAMPLES FOR THE ROSIS-03 PAVIA UNIVERSITY DATASET

Class	Class name	#Training	#Test	#Total
C1	Asphalt	200	6431	6631
C2	Meadows	200	18449	18649
C3	Gravel	200	1899	2099
C4	Trees	200	2864	3064
C5	Metal Sheets	200	1145	1345
C6	Bare Soil	200	4829	5029
C7	Bitumem	200	1130	1330
C8	Bricks	200	3482	3682
C9	Shadow	200	747	947
Total	-	1800	40976	42776

TABLE III
THE CLASSIFICATION RESULTS OF SVM [8], S-CNN[38], GABOR-CNN [39], DFFN [40], 3D-GAN [51] AND FREENET ON THE ROSIS-03 PAVIA UNIVERSITY DATASET.

Class		Patch-based					Patch-free
		SVM	S-CNN	Gabor-CNN	DFFN	3D-GAN	FreeNet
Accuracy(%)	C1	85.49	95.47	99.53	99.53	99.18	99.58
	C2	92.12	98.71	98.21	97.71	98.86	99.88
	C3	85.77	97.32	89.74	99.89	94.94	99.95
	C4	96.41	97.72	93.02	97.88	90.15	99.27
	C5	98.60	100	99.42	99.48	99.49	100
	C6	92.52	97.67	98.77	99.69	98.56	100
	C7	93.79	98.36	98.82	100	92.74	100
	C8	86.56	95.56	94.12	98.59	97.18	99.83
	C9	97.97	100	97.91	99.61	98.51	100
OA(%)		90.78	97.93	97.33	98.57	97.81	99.81
AA(%)		92.14	97.88	96.62	99.16	96.65	99.83
Kappa		0.8813	0.9743	0.9662	0.9808	0.9697	0.9974

LITERATURE SURVEY - IV

Title: Dual Graph Convolutional Network for Hyperspectral Image Classification With Limited Training Samples

Author(s): Xin He , Yushi Chen ,Member, IEEE, and Pedram Ghamisi ,Senior Member, IEEE

Summary of Dual Graph Convolutional Networks for HIC

- A DGCN, which is a hybrid network of CNN and two graph networks (i.e., the **point graph** and the **distribution graph**), is proposed for HSI classification **with limited training samples**
- Instead of simply applying GCN to classify HSI, the **point graph** aims to fully explore the relationships among samples, and the **distribution graph** utilizes label distribution learning to obtain high correlation features among samples with the same label. The two graphs are integrated with each other to fully extract features among training samples
- In order to mitigate the **overfitting issue** caused by limited HSI training samples, **the drop edge** is investigated in the proposed DGCN
- To further improve the HSI classification results, motivated by the regularization method called **cutout**, we propose a novel technique by improving the cutout with the **multiscale operation to feature maps** in CNN; this method **increases the generalization capability** of the proposed DGCN

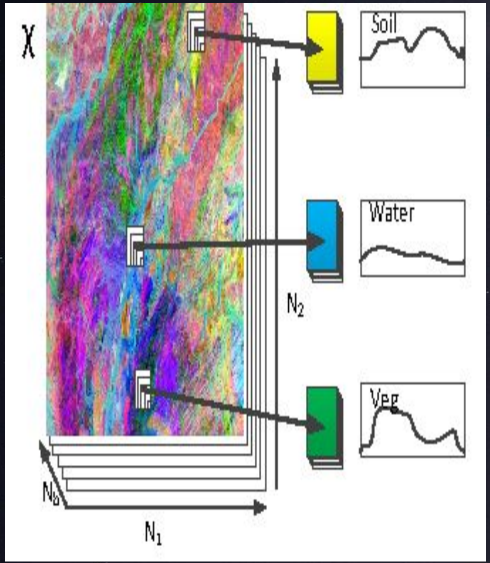

LITERATURE SURVEY - IV

DGCN for HSI Classification

DGCN-D

DGCN

DGCN-M

Data Set(s)

- Indian Pines
- Pavia University
- Houston University
- Salinas Dataset

The flow diagram of SSDGL Framework

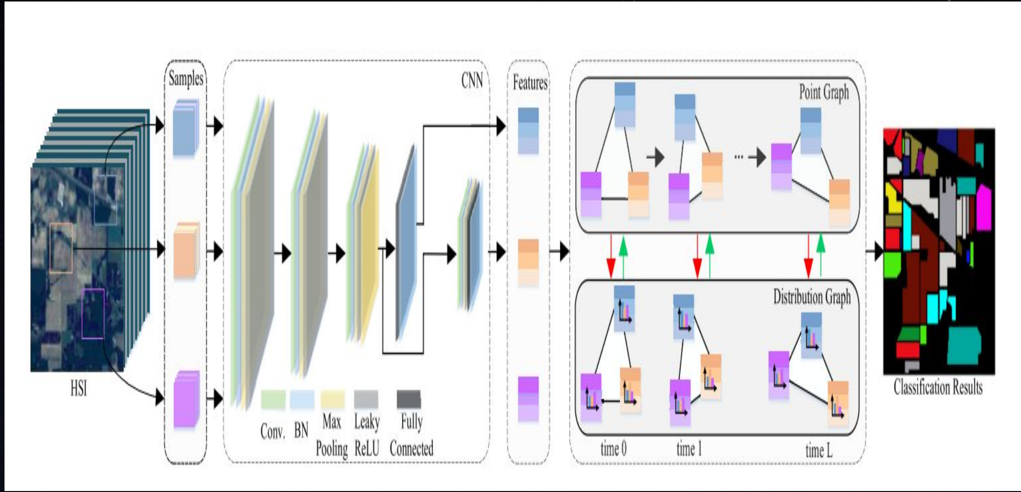

Observation

Pavia

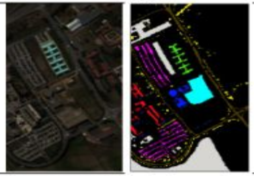

Class No.	Class Color	Class Name	Sample Number
1		Asphalt	6852
2		Meadows	18686
3		Gravel	2207
4		Trees	3436
5		Metal sheets	1378
6		Bare soil	5104
7		Bitumen	1356
8		Bricks	3878
9		Shadow	1026

CLASSIFICATION RESULTS (VALUES ± STANDARD DEVIATION) ON THE PAVIA DATA SET USING FIVE TRAINING SAMPLES PER EACH CLASS

Method	EMP-SVM	CNN	EMP-CNN	SCNN	HySN	GCN	**DGCN**	**DGCN-D**	**DGCN-C**	**DGCN-M**	**DGCN-DC**
OA(%)	74.71±3.39	69.42±2.41	74.01±4.51	69.01±6.11	65.76±4.32	65.12±2.73	75.60±6.00	77.21±4.49	78.28±3.36	78.40±4.24	**79.87±5.74**
AA(%)	77.22±2.91	71.91±2.29	75.75±4.08	68.89±5.32	65.99±3.91	67.51±1.85	77.05±5.98	79.80±4.47	78.46±3.35	78.43±4.73	**79.84±5.81**
K×100	71.45±3.81	65.47±2.72	70.67±5.07	65.21±8.08	61.26±4.86	60.56±3.03	72.75±6.77	74.26±5.07	75.46±3.77	75.61±4.78	**77.09±6.52**
Asphalt	71.87±10.58	56.50±5.91	54.38±9.78	65.94±5.05	37.43±20.27	60.15±13.79	76.10±5.50	**79.65±4.22**	77.15±2.87	78.16±4.04	78.99±3.62
Meadows	65.36±21.95	69.71±12.50	77.65±12.66	**81.62±3.23**	74.10±13.18	27.22±9.14	76.70±7.11	78.90±5.05	76.85±3.89	77.66±5.18	80.91±4.72
Gravel	49.25±11.06	39.51±10.88	39.88±23.29	28.98±12.78	**82.86±18.29**	50.48±21.65	77.40±5.91	80.90±4.45	79.25±2.96	79.12±4.63	79.43±4.02
Trees	**89.87±10.27**	89.61±5.61	77.76±16.43	73.26±5.18	60.18±18.73	80.35±10.18	76.50±5.79	79.60±4.47	77.85±2.70	78.15±4.82	79.23±4.16
Metal sheets	**98.18±1.04**	90.93±5.41	92.77±4.22	75.20±2.41	94.81±7.56	96.87±1.39	78.74±6.60	80.33±4.85	77.58±4.03	78.42±5.17	80.79±4.07
Bare soil	77.37±21.03	58.81±6.28	79.35±11.31	73.99±4.07	71.17±26.24	**96.69±29.03**	77.35±5.88	80.15±4.20	79.65±3.56	79.11±4.88	81.03±3.55
Bitumen	88.82±6.23	76.61±9.90	87.16±4.73	77.86±8.61	**97.57±2.85**	49.37±13.71	76.25±5.94	78.54±4.67	80.16±3.59	78.70±5.12	80.60±4.41
Bricks	75.26±12.57	68.78±8.60	**87.46±4.81**	61.76±2.45	49.73±22.57	47.22±29.92	75.70±6.20	80.75±4.72	79.55±4.32	78.28±5.18	79.30±4.16
Shadow	97.73±1.47	96.72±1.40	85.33±9.71	81.37±7.27	26.10±14.59	**99.22±1.01**	78.75±5.46	79.34±3.86	78.36±3.12	78.28±4.35	78.33±4.83
Training Time (sec.)	4.67	7.13	3.28	357.42	11.33	85.92	260.95	195.20	536.63	388.12	449.25
Test Time (sec.)	0.07	47.74	6.56	883.79	111.53	6.68	164.50	140.91	167.92	125.55	110.42

LITERATURE SURVEY - V

Title: A Spectral-Spatial Dependent Global Learning Framework for Insufficient and Imbalanced Hyperspectral Image Classification

Author(s): Qiqi Zhu, Weihuan Deng, Zhuo Zheng, Yanfei Zhong, Senior Member, IEEE, Liangpei Zhang, IEEE, Deren Li, IEEE

Summary of Spectral-Spatial Dependent Global Framework

- Spectral-Spatial Dependent Global Learning (SSDGL), combines spectral and spatial information to learn global discriminative features for classification
- The framework includes three modules: a spectral-spatial dependent feature extraction module, a global feature learning module, and a classification module.
- The experimental results show that the SSDGL framework outperforms existing methods in terms of accuracy, especially when dealing with insufficient and imbalanced data

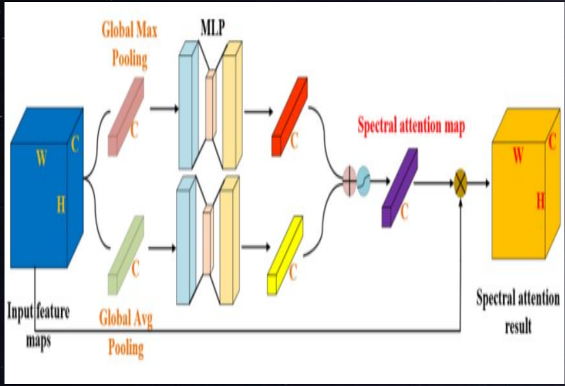

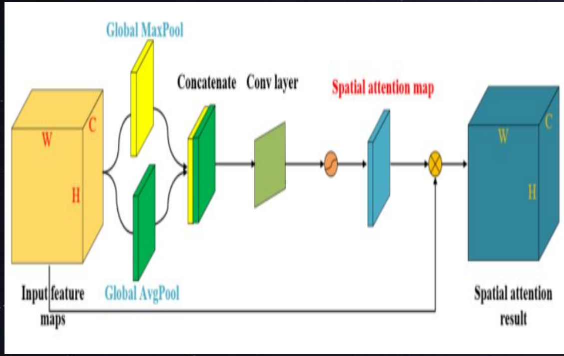

LITERATURE SURVEY - V

Data Set(s)

- Indian Pines Dataset
- Pavia University Dataset
- Houston University Dataset

The flow diagram of SSDGL Framework

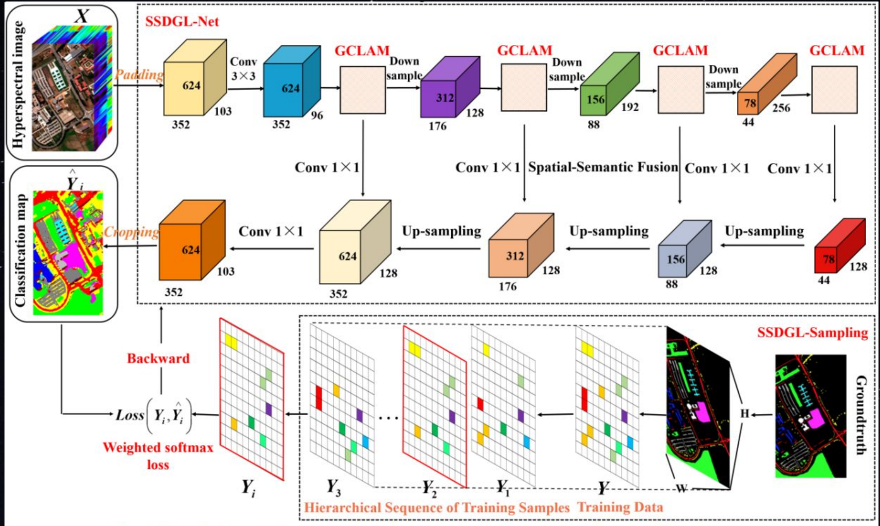

Fig. 2. Flowchart of insufficient and imbalanced HSI classification based on the SSDGL framework.

Observation

THE NUMBER OF TRAINING SAMPLES AND TEST SAMPLES FOR THE INDIAN PINES DATASET

No.	Class.	Train.	Test.	Total.
1	Alfalfa	5	41	46
2	Corn-notill	72	1356	1428
3	Corn-mintill	42	788	830
4	Corn	12	225	237
5	Grass-pasture	25	458	483
6	Grass-trees	37	693	730
7	Grass-pasture-mowed	5	23	28
8	Hay-windrowed	24	454	478
9	Oats	5	15	20
10	Soybean-notill	49	923	972
11	Soybean-mintill	123	2332	2455
12	Soybean-clean	30	563	593
13	Wheat	11	194	205
14	Woods	64	1201	1265
15	Buildings-Grass-Trees	20	366	386
16	Stone-Steel-Towers	5	88	93
	Total	529	9720	10249

THE CLASSIFICATION RESULTS OF RBF-SVM, SS-CNN, SSRN, DBMA, MCNN-CONVLSTM, U-NET, FPGA AND SSDGL ON THE INDIAN PINES DATASET WITH 5% LABELED SAMPLES.

Class	CNN-based					FCN-based		
	RBF-SVM	SS-CNN	SSRN	DBMA	MCNN-CONVLSTM	U-Net	FPGA	Proposed
1	70.32	72.14	75.57	90.37	94.36	97.67	97.22	**100.00**
2	69.63	90.42	90.65	92.72	92.84	92.48	93.07	**99.63**
3	58.26	81.48	97.01	95.63	93.02	84.77	89.46	**99.24**
4	45.22	71.23	93.36	89.35	95.32	89.33	100.00	**100.00**
5	75.48	83.62	98.56	96.92	92.13	81.00	95.63	**99.56**
6	96.14	97.19	98.94	99.18	98.86	94.08	97.56	**100.00**
7	95.79	91.03	84.21	79.57	84.83	100.00	100.00	**100.00**
8	87.72	92.34	98.36	99.11	98.63	98.90	100.00	**100.00**
9	75.03	96.39	97.61	97.91	92.47	78.95	100.00	**100.00**
10	66.25	81.75	81.03	92.08	94.76	89.49	96.64	**99.68**
11	77.62	87.39	93.02	95.15	96.28	97.81	96.74	**99.36**
12	67.28	83.03	95.72	90.71	94.12	86.50	91.65	**99.11**
13	96.93	97.42	99.81	99.81	96.95	98.97	100.00	**100.00**
14	95.07	95.31	95.79	97.11	98.79	98.58	99.91	**100.00**
15	35.48	74.04	92.25	88.13	92.83	92.08	99.72	**100.00**
16	97.61	94.61	96.57	97.05	87.32	93.18	100.00	**100.00**
OA	75.31	89.82	92.21	94.43	94.78	93.20	96.18	**99.63**
AA	71.12	83.73	93.03	93.81	93.37	92.11	97.33	**99.79**
Kappa	0.7173	0.8783	0.9115	0.9365	0.9437	0.9222	0.9564	**0.9958**

IMPLEMENTATION

Before working on the Chandrayaan-2 dataset, we decided to work on Cuprite Dataset which is considered as benchmark for hyperspectral unmixing.

Information about cuprite dataset:-

- No. of bands: 224

Wavelength range: 370-2480nm

No. of end members: Actually 14 but there are minor differences between variants of similar minerals so 12 end members are considered.

Spectral resolution: 10nm

Spatial resolution: 20m

IMPLEMENTATION

Airborne Visible/Infrared Imaging Spectrometer (AVIRIS) sensor was used to capture the cuprite data

Information about AVIRIS sensor:-

- Aircraft used: NASA's ER-2

Speed of Aircraft: 730 kmph

Altitude: 20km

Location: Cuprite mining district, Nevada, U.S

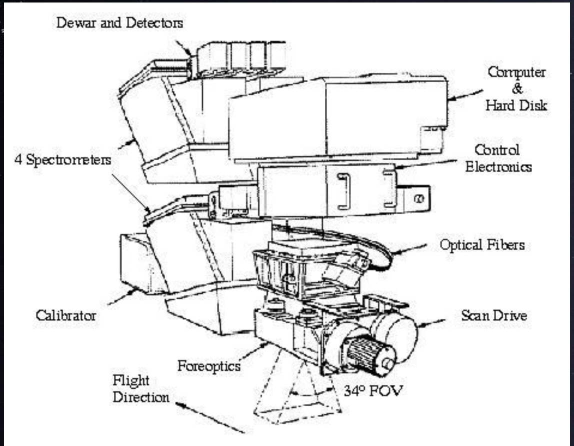

IMPLEMENTATION

Pre-processing of Cuprite Data

As the cuprite dataset is unlabelled, we have pre-processed the data and took few labelled data points using which we can predict the labels of other unlabelled data points with the help of various deep learning models.

- Labels of Cuprite data

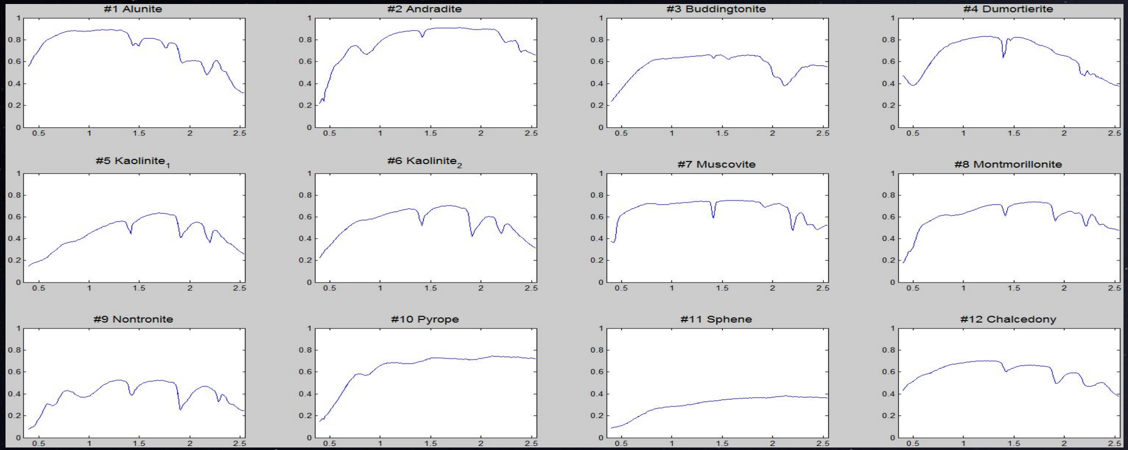

IMPLEMENTATION

Implementing 1D-CNN on pre-processed cuprite data

We have implemented 1D CNN on the ~1000 data points extracted during the pre-processing.

Results

```
Confusion Matrix:
 [[16  0  0  0  0  1  0  0  1  0  0  0]
 [ 0 21  0  0  0  0  0  1  0  2  0  0]
 [ 0  0  8  0  0  0  2  0  0  0  0  0]
 [ 0  0  0 13  1  3  0  0  0  0  0  0]
 [ 0  1  0  0 32  0  0  0  2  0  0  0]
 [ 0  0  0  0  0 11  0  0  3  0  0  0]
 [ 1  0  0  1  0  0  9  2  0  0  0  0]
 [ 0  3  1  1  0  1  1 18  0  0  0  1]
 [ 0  1  0  0  0  0  0  0 58  0  0  0]
 [ 0  0  0  0  0  0  0  0  0 45  0  0]
 [ 0  0  0  0  0  0  0  0  0  6 37  0]
 [ 0  0  0  1  0  1  2  1  0  0  0  6]]
Accuracy: 0.8698412698412699
Precision: 0.845041823529268
Recall: 0.816848388754038
F1-score: 0.8254094805359907
ROC AUC score: 0.977411523233787
```

IMPLEMENTATION

Predicted labels of Cuprite data by 1D CNN:

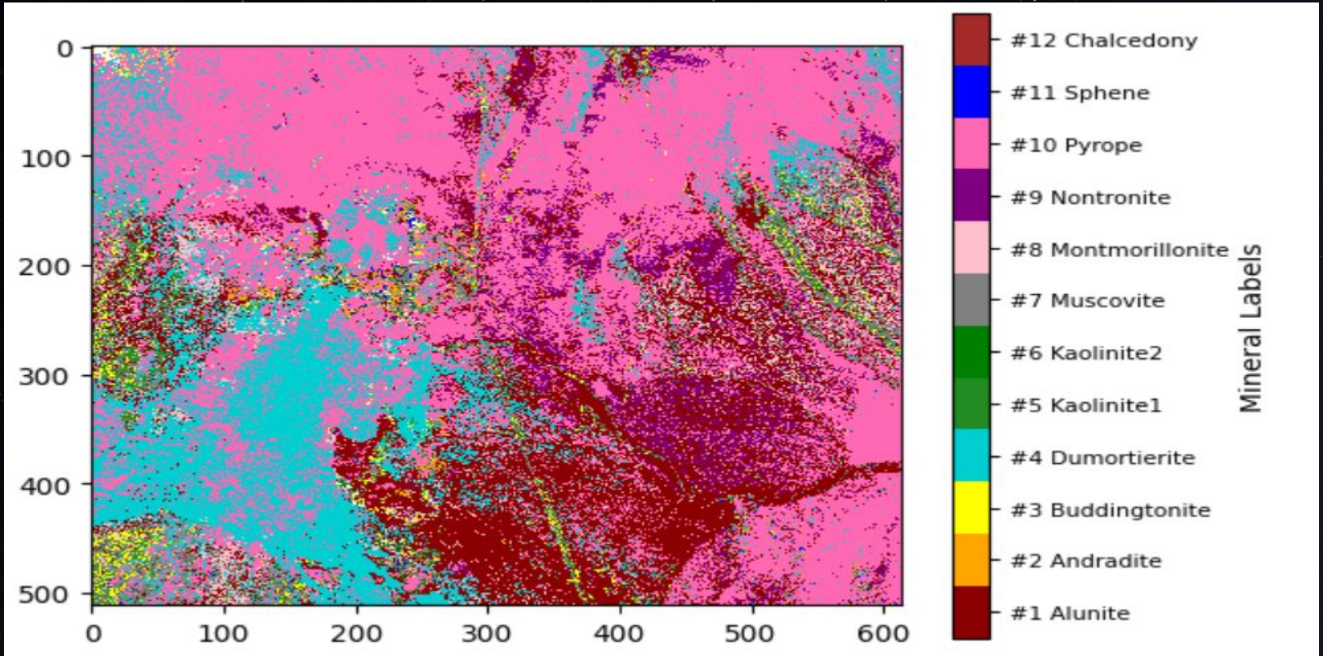

IMPLEMENTATION

Implementing 2D-CNN on pre-processed cuprite data

We have implemented 2D CNN on the ~1000 data points extracted during the pre-processing.

Results

```
Confusion Matrix:
 [[16  0  0  0  0  2  0  0  0  0  0  0]
 [ 0 21  0  0  0  0  0  1  0  1  1  0]
 [ 0  1  6  0  0  0  2  1  0  0  0  0]
 [ 0  0  0 11  0  5  0  1  0  0  0  0]
 [ 0  0  0  0 33  0  0  0  2  0  0  0]
 [ 0  0  0  0  0 12  0  0  2  0  0  0]
 [ 1  0  0  0  0  0  8  3  0  0  0  1]
 [ 0  0  0  1  0  1  0 24  0  0  0  0]
 [ 0  0  0  0  0  0  0  1 58  0  0  0]
 [ 0  0  0  0  0  0  0  0  0 43  2  0]
 [ 0  0  0  0  0  0  0  0  0  1 42  0]
 [ 0  0  0  0  0  1  0  0  1  0  0  9]]
Accuracy: 0.8984126984126984
Precision: 0.8889612100949863
Recall: 0.8402451381767793
F1-score: 0.8540061149713427
ROC AUC score: 0.9868236470641417
```

IMPLEMENTATION

Predicted labels of Cuprite data by 2D CNN:

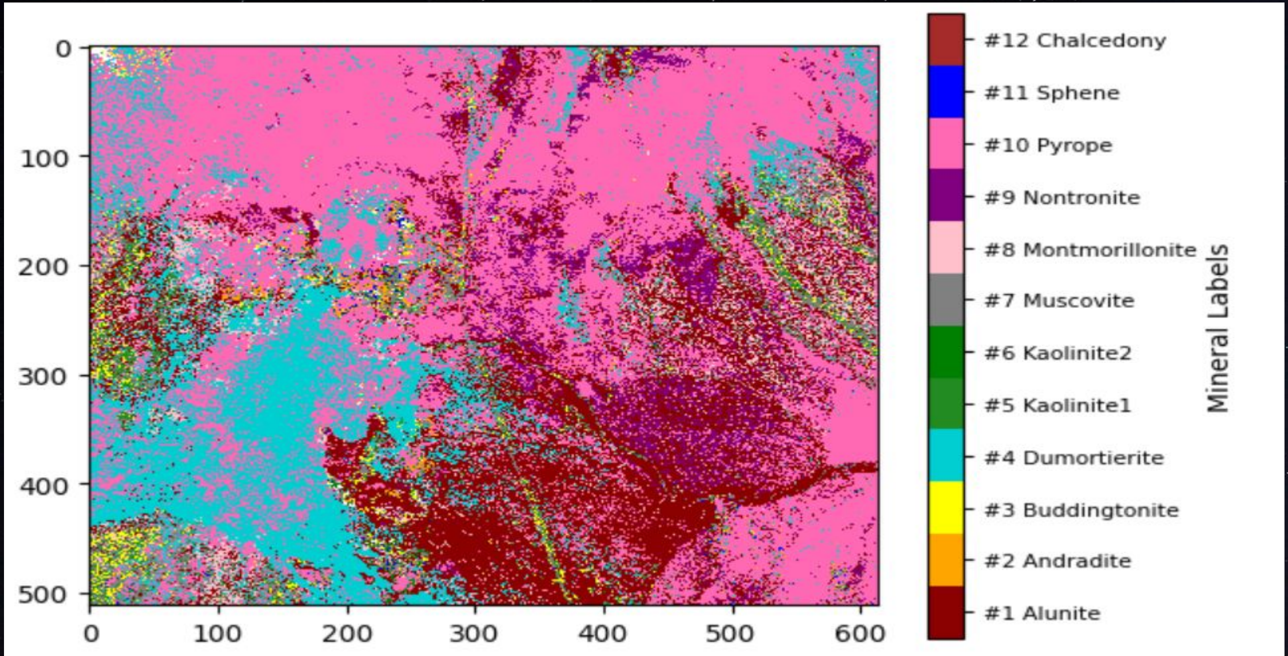

IMPLEMENTATION

Implementing HybridSN on pre-processed Cuprite Dataset (1051 samples)

Initially, we have extracted 1051 samples by pre-processing the Cuprite dataset and implemented HybridSN on it.

Results

	precision	recall	f1-score	support
0	0.22	0.14	0.17	28
1	0.25	0.11	0.15	9
2	0.38	0.38	0.38	16
3	0.83	0.86	0.85	35
4	0.10	0.07	0.08	15
5	0.53	0.67	0.59	15
6	0.30	0.11	0.16	27
7	0.51	0.79	0.62	56
8	0.69	0.87	0.77	47
9	0.85	0.80	0.83	41
10	1.00	0.11	0.20	9
accuracy			0.58	298
macro avg	0.51	0.45	0.44	298
weighted avg	0.56	0.58	0.55	298

IMPLEMENTATION

Implementing HybridSN on pre-processed Cuprite Dataset (4812 samples)

As the accuracy was poor with 1000 samples, we have extracted 4812 samples by pre-processing the Cuprite dataset again and implemented HybridSN on it.

- ## Results

	precision	recall	f1-score	support
0	0.88	0.88	0.88	121
1	0.50	0.54	0.52	120
2	0.57	0.62	0.59	120
3	0.74	0.74	0.74	121
4	0.78	0.73	0.76	120
5	0.74	0.74	0.74	120
6	0.48	0.45	0.46	120
7	0.72	0.78	0.75	120
8	0.69	0.60	0.64	121
9	0.70	0.76	0.73	120
10	0.66	0.68	0.67	120
11	0.55	0.50	0.53	121
accuracy			0.67	1444
macro avg	0.67	0.67	0.67	1444
weighted avg	0.67	0.67	0.67	1444

IMPLEMENTATION

Implementing HybridSN on pre-processed Cuprite Dataset (12012 samples)

Even with 4000 samples the accuracy wasn't satisfactory, so we have extracted 12012 samples by pre-processing the Cuprite dataset again and implemented HybridSN on it.

- ## Results

113/113 [==============================] - 28s 244ms/step

	precision	recall	f1-score	support
0	0.99	1.00	1.00	301
1	0.97	0.99	0.98	300
2	0.98	0.98	0.98	300
3	0.99	0.97	0.98	301
4	1.00	0.99	0.99	300
5	0.99	0.97	0.98	300
6	0.97	0.99	0.98	300
7	0.99	1.00	0.99	300
8	0.98	0.95	0.96	301
9	0.95	0.97	0.96	300
10	0.97	0.99	0.98	300
11	0.99	0.98	0.99	301
accuracy			0.98	3604
macro avg	0.98	0.98	0.98	3604
weighted avg	0.98	0.98	0.98	3604

IMPLEMENTATION

Implementing HybridSN on Indian Pines Dataset

We have implemented HybridSN on the Indian Pines dataset.

Results

```
8.0268032848835 Test loss (%)
97.40766286849976 Test accuracy (%)

97.04344405901733 Kappa accuracy (%)
97.4076655052648 Overall accuracy (%)
91.5002867214762 Average accuracy (%)
```

CONCLUSION

Why only CNN ?

- Compare to other methods like GCN the computational complexity of CNN is less
- The Convolution filter can capture can capture high dimensional image data in an effective way without loss of information

1D CNN vs 2D CNN vs 3D CNN

- 1D CNN captures only spectral data
- 2D CNN captures only spatial data
- 3D CNN captures both spatial and spectral data but computational cost is high when compared to 1D and 2D CNN
- HybridSN just like 3D CNN captures both spatial and spectral data but computational cost is less compared to 3D CNN

LITERATURE SURVEY

Title: A CNN with Noise Inclined Module and Denoise Framework for Hyperspectral Image Classification

Author(s): Zhiqiang Gong, Ping Zhong, Senior Member, IEEE, Jiahao Qi, and Panhe Hu

Summary of CNN with Noise Inclined Module and Denoise Framework for HSI

- Most of prior works adopt general deep architectures while ignore the intrinsic structure of the hyperspectral image, such as the physical noise generation.
- To leverage such intrinsic information, this work develops a novel deep learning framework with the noise inclined module and denoise framework for hyperspectral image classification
- The experimental results show that this framework outperforms existing methods in terms of accuracy, and is more effective in generating discriminative features.

ARCHITECTURE

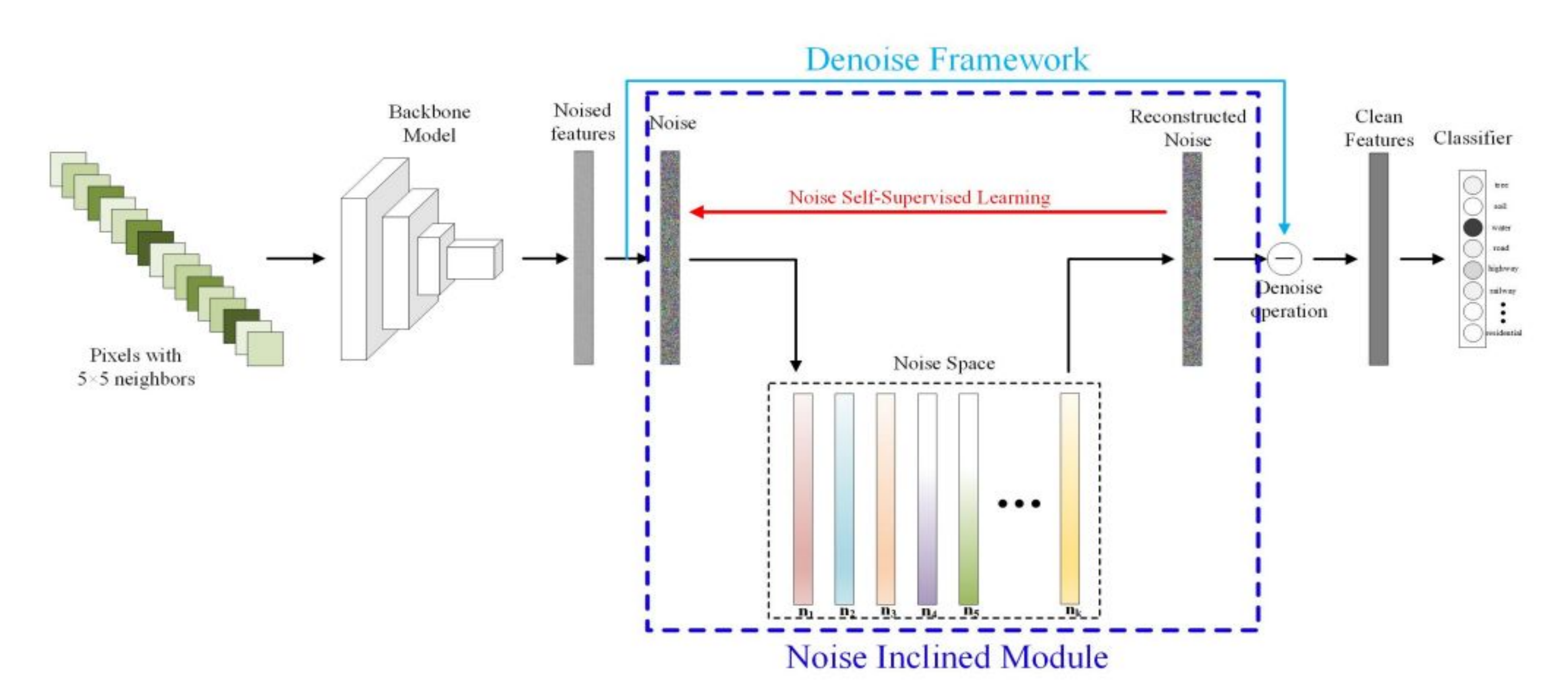

IMPLEMENTATION

Implementing Noise Inclined module and Denoise framework on Pavia University Dataset

Results

```
PS C:\Users\Lenovo\Desktop\noise-physical-framework-master\noise-physical-framework-master> python main.py --method NoiPhy
 --dataset pavia --neighbor 5 -e
Starting......
Prepared dataset, train:36878,           val:4098, test:40976

Evaluation only
checkpoint/model_best.pth.tar
 Test Loss:  0.36720554, Test Acc:  89.29
```

LITERATURE SURVEY

Title: Morphological Convolutional Neural Networks for Hyperspectral Image Classification

Author(s): Swalpa Kumar Roy, Student Member, IEEE, Ranjan Mondal, Mercedes E. Paoletti, Senior Member, IEEE, Juan M. Haut, Senior Member, IEEE, and Antonio Plaza, Fellow, IEEE

Summary of Morphological Convolution Neural Networks for Hyperspectral Image Classification

- Morphological operations are powerful nonlinear transformations for feature extraction that preserve the essential characteristics of the image, such as borders, shape and structural information.
- The method includes spectral and spatial morphological blocks to extract relevant features from the HSI input data.
- The experimental results show that this framework outperforms existing traditional methods of 2D and 3D CNN

ARCHITECTURE

-

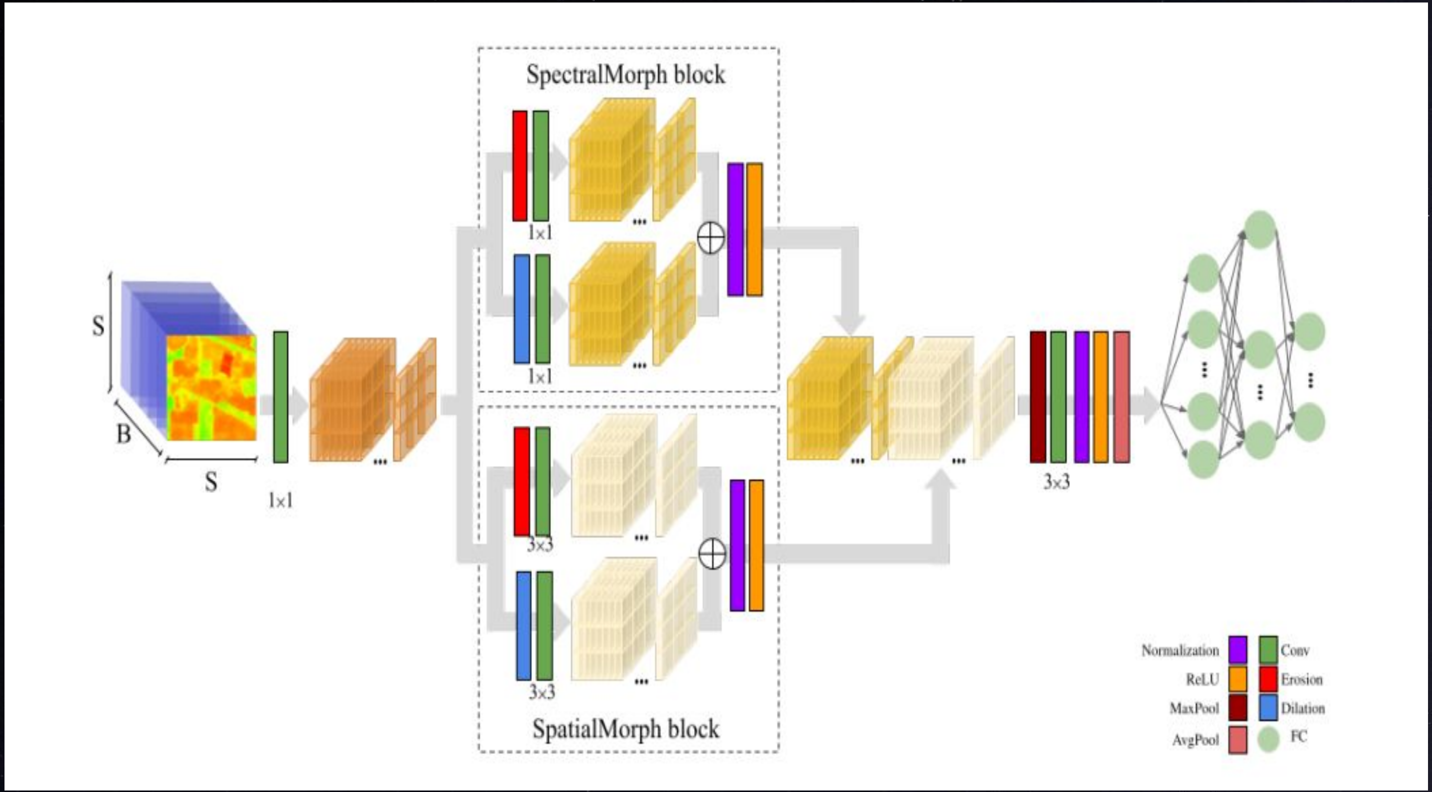

IMPLEMENTATION

Implementation on Pavia University dataset

	precision	recall	f1-score	support
0	0.90	0.57	0.70	3149
1	0.97	0.74	0.84	7353
2	0.00	0.00	0.00	0
3	0.00	0.00	0.00	0
4	0.41	0.90	0.56	189
5	0.31	0.41	0.35	1148
6	0.00	0.00	0.00	0
7	0.53	0.61	0.57	994
8	0.00	0.00	0.00	0
accuracy			0.66	12833
macro avg	0.35	0.36	0.33	12833
weighted avg	0.85	0.66	0.73	12833

LITERATURE SURVEY

Title: Accelerating Convolutional Neural Network-Based Hyperspectral Image Classification by Step Activation Quantization

Author(s): Shaohui Mei , Senior Member, IEEE, Xiaofeng Chen, Yifan Zhang , Member, IEEE, Jun Li , Fellow, IEEE, and Antonio Plaza , Fellow, IEEE

Summary of Accelerating Convolutional Neural Network-Based Hyperspectral Image Classification by Step Activation Quantization

- In this article, a new step activation quantization method is proposed to constrain the input of the network layer of the CNN so that the data can be represented by low-bit integers.
- As a result, floating-point operations are replaced with integer operations to greatly accelerate the forward (inference) step of the network.
- The proposed step activation quantization acceleration method is applied to a CNN for HSI with two well-known benchmark data sets and the experimental results demonstrate that the proposed method is very effective.

IMPLEMENTATION

Implementation on Pavia University dataset

```
logs_pavia/SAWB-C-dorefa_1w2a_0.01_0.0005_64_200_[100, 150, 200]
current lr 1.00000e-03, using gpu : 0
Epoch: [123][0/29]      Time 1.801 (1.801)      Data 1.652 (1.652)       Loss 0.1992 (0.
1992)    OA 89.062 (89.062)
Epoch: [123][5/29]      Time 0.186 (0.412)      Data 0.000 (0.276)       Loss 0.1128 (0.
1675)    OA 96.875 (92.188)
Epoch: [123][10/29]     Time 0.119 (0.280)      Data 0.000 (0.151)       Loss 0.2658 (0.
1609)    OA 85.938 (92.898)
Epoch: [123][15/29]     Time 0.123 (0.231)      Data 0.000 (0.104)       Loss 0.2100 (0.
1513)    OA 95.312 (93.750)
Epoch: [123][20/29]     Time 0.117 (0.204)      Data 0.000 (0.079)       Loss 0.1747 (0.
1491)    OA 92.188 (93.973)
Epoch: [123][25/29]     Time 0.117 (0.188)      Data 0.001 (0.064)       Loss 0.0832 (0.
1548)    OA 98.438 (93.870)
Test: [0/321]   Time 3.638 (3.638)      Loss 0.2008 (0.2008)      OA 91.406 (91.406)
Test: [50/321]  Time 0.128 (0.205)      Loss 0.0783 (0.2005)      OA 97.656 (93.382)
Test: [100/321] Time 0.128 (0.168)      Loss 0.2099 (0.1743)      OA 95.312 (94.570)
Test: [150/321] Time 0.131 (0.155)      Loss 0.1634 (0.1560)      OA 96.094 (95.256)
Test: [200/321] Time 0.127 (0.149)      Loss 0.1881 (0.1625)      OA 89.062 (94.543)
Test: [250/321] Time 0.143 (0.145)      Loss 0.2196 (0.1802)      OA 95.312 (93.753)
Test: [300/321] Time 0.135 (0.143)      Loss 0.0403 (0.1712)      OA 100.000 (94.316)
correct_per_class: [ 5806. 17620.  1628.  2727.  1145.  4756.  1115.  3256.   717.]
sample_per_class: [ 6431. 18449.  1899.  2864.  1145.  4829.  1130.  3482.   747.]
 * OA 94.616

 * AA 94.821
```

Combination of Morphological CNN with Noise inclined module and denoising framework:

- Based on our implementations we have found that morphological CNN works better than traditional CNN methods.
- Noise inclined module concentrates on denoising the data.
- The combination of these two can yield us effective results.
- So we have decided it to propose it as out novel approach.

Combination of Morphological CNN with Noise inclined module and denoising framework:

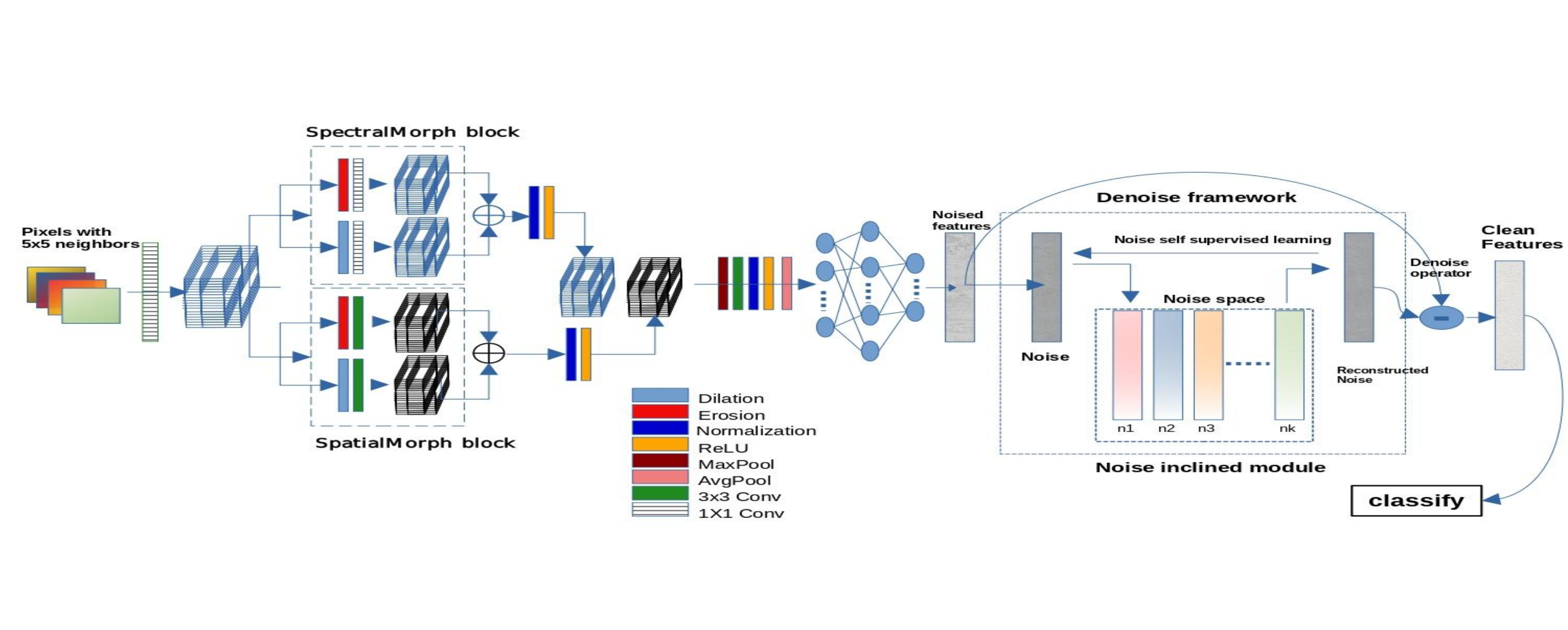

OUR NOVEL APPROACH

Accelerating HybridSN with dynamic step quantization:

- HybridSN was proven to be effective in classifying complex HSI data.
- It leverages the benefits of both 3D-CNN and 2D-CNN there by reducing the computational cost.
- Still significant amount of computational complexity persists in the implementation of HybridSN.
- To address this we are proposing a novel dynamic step quantization method to accelerate the HybridSN framework.

OUR NOVEL APPROACH

Phase I: Re-construction of HybridSN architecture with binary weights

- The diverse floating point weights of HybridSN model are replaced by binary weights (typically -1 and 1).
- Reconstructing model with binary weights have several advantages such as reduced computation, faster model loading, improved robustness etc.,
- On the flipside, binarizing weights leads to significant amount of loss in the accuracy.
- To overcome this, the absolute mean of real weights is used as a scaling factor thereby reducing the loss in the accuracy.

Architecture of HybridSN

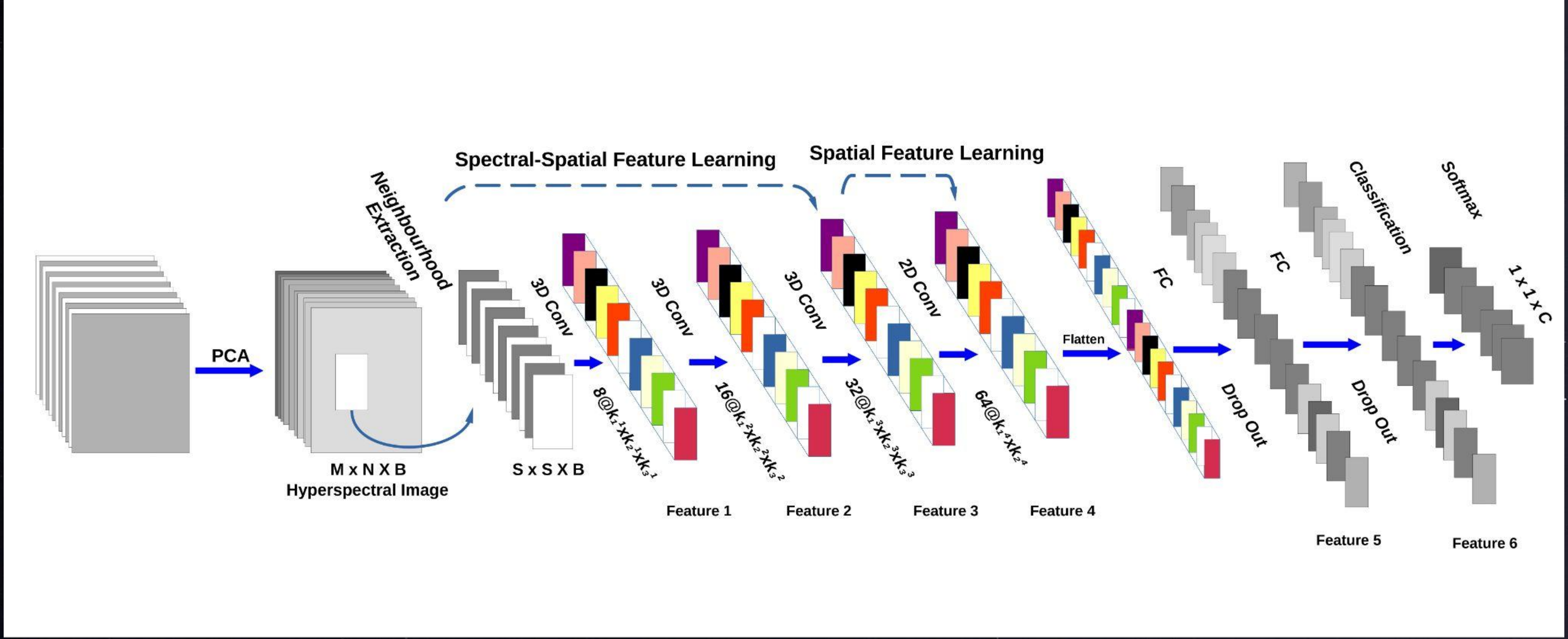

OUR NOVEL APPROACH

Phase II: Using dynamic step quantization for accelerating the reconstructed HybridSN model

- Step Activation Quantization (SAQ) is proven to accelerate the inference speed of convolutional neural networks (CNNs) for hyperspectral image (HSI) classification.
- But having a fixed value for the precision of bits after quantization for all the layers is not an effective approach.
- In this regard, we are proposing a novel approach of dynamic quantization where the precision for each layer is dynamically updated at each epoch reducing the quantization loss thereby improving accuracy.

DataSets Evaluated

The Pavia University dataset is a renowned hyperspectral image dataset captured by the Reflective Optics System Imaging Spectrometer (ROSIS) sensor. It focuses on the Pavia region in Italy and includes 115 spectral bands. This high-dimensional data provides detailed information about the urban landscape, featuring various urban materials, such as buildings, roads, trees, and other surfaces. The dataset is widely used in remote sensing research for tasks like classification, target detection, and land cover analysis, offering rich insights into urban environments and aiding in the development of algorithms for image processing and analysis.

Pavia University DataSet

#	Class	Samples	Training	Validation	Test
1	Asphalt	6631	3979	1326	1326
2	Meadows	18,649	11,189	3730	3730
3	Gravel	2099	1259	420	420
4	Trees	3064	1838	613	613
5	Painted metal sheets	1345	807	269	269
6	Bare Soil	5029	3017	1006	1006
7	Bitumen	1330	798	266	266
8	Self-blocking bricks	3682	2210	736	736
9	Shadows	947	569	189	189
Total		42,776	25,666	8555	8555

DataSets Evaluated

Indian Pines Dataset

The Indian Pines dataset is a widely used remote sensing dataset in the field of hyperspectral image analysis. It comprises aerial imagery collected by an AVIRIS sensor over the Indian Pines agricultural site in northwestern Indiana, USA. The dataset contains 16 classes of land cover, including various crops, trees, and bare soil. With 220 spectral bands, it enables detailed analysis for tasks like classification, land cover mapping, and vegetation studies, making it a valuable resource for remote sensing and machine learning research.

Class Number	No. of Samples	Classification
1	46	Alfalfa
2	1428	Corn-notill
3	830	Corn-mintill
4	237	Corn
5	483	Grass-pasture
6	730	Grass-trees
7	28	Grass-pasture
8	478	Hay-windrowed
9	20	Oats
10	972	Soybean-notill
11	2455	Soybean-mintill
12	593	Soybean-clean
13	205	Wheat
14	1265	Woods
15	386	Building-grass-trees-drives
16	93	Stone-steal-towers
Total	10,249	

Figure 2: Classification and Sample Counts of Indian pines DataSet

Classification Results

HybridSN

Here are the results of the implementation of HybridSN: A 3D-2D CNN feature hierarchy on Indian Pines and University of Pavia datasets.

Methods	Indian Pines Dataset		University of Pavia Dataset	
	OA (%)	AA (%)	OA (%)	AA (%)
SVM	85.30 ± 2.8	79.03 ± 2.7	94.34 ± 0.2	92.98 ± 0.4
2DCNN	89.48 ± 0.2	86.14 ± 0.8	97.86 ± 0.2	96.55 ± 0.0
3DCNN	91.10 ± 0.4	91.58 ± 0.2	96.53 ± 0.1	97.57 ± 1.3
M3DCNN	95.32 ± 0.1	96.41 ± 0.7	95.76 ± 0.2	95.08 ± 1.2
SSRN	99.19 ± 0.3	98.93 ± 0.6	99.90 ± 0.0	99.91 ± 0.0
HybridSN	99.75 ± 0.1	99.63 ± 0.2	99.98 ± 0.0	99.97 ± 0.0

Figure 4: Classification Accuracies on Indian Pines, University of Pavia Datasets using HybridSN and state-of-the-art methods.

Classification Results

Step Activation Quantization (SAQ) to accelerate convolutional neural networks (CNNs) for hyperspectral image (HSI) classification. SAQ quantizes activation values to low-bit integers, leading to faster inference speed with minimal loss in accuracy. It achieves up to 10 times acceleration on benchmark HSI datasets, paving the way for deploying CNN-based HSI classification in real-world applications.

Accelerating CNN (Step Activation)

Class	Label	Training	Testing	Benchmark-CNN	SAWB-C	SAWB-T
Water	1 2	200	65771	99.99	99.99	99.99
Trees	3 4	200	7398	98.00	99.22	99.58
Asphalt	5 6	200	2890	98.38	93.27	83.73
Bricks	7 8	200	2485	99.99	99.03	97.42
Bitumen	9	200	6384	97.59	98.01	97.73
Tiles		200	9048	98.53	96.99	98.15
Shadows		200	7087	99.44	97.50	95.67
Meadows		200	42626	99.13	99.15	99.36
Bare Soil		200	2663	97.82	97.41	97.30
AA(%)		/	/	/	98.76	(10.92)
OA (%)		/	/	/	99.35	(10.23)

Figure 3: Class-specific Accuracies, OA, and AA on the Pavia dataset (Step Activation Quantization)

Classification Results

Our Proposed Methodology

The improved performance of the HybridSN-Binary model with dynamic step quantization can be attributed to the combined effects of binary weights, dynamic step quantization, and the effective architecture of the HybridSN model. Binary weights significantly reduce computational complexity and memory requirements, making the model suitable for resource-constrained environments. Dynamic step quantization further enhances the model's accuracy by reducing quantization noise and preserving more information in the reduced precision representations.

Class Label	Training	Testing	Proposed Model
1	200	65771	99.99
2	200	7398	98.00
3	200	2890	98.38
4	200	2485	99.99
5	200	6384	97.59
6	200	9048	98.53
7	200	7087	99.44
8	200	42626	99.13
9	200	2663	97.82
10	200	2663	97.82
11	200	2663	97.82
12	200	2663	97.82
13	200	2663	97.82
14	200	2663	97.82
15	200	2663	97.82
16	200	2663	97.82
OA (%)	/	/	99.2

Figure 5: Class-specific Accuracies, OA, and AA on the Indian Pines Dataset (our proposed method)

07

TIMELINE

TIMELINE

Sem - 6	Phase 1	Exploring the deep learning and neural networks
	Phase 2	Working on Preprocessing of Hyperspectral data
	Phase 3	Understanding the methodologies for mapping of Lunar Surface data using Hyperspectral Image classification
Sem - 7	Phase 4	Image classification for hyperspectral data on the chandrayaan 2 IIRS dataset.
	Phase 5	SARS
Sem - 8	Phase 6	To work and publish the novel approach

REFERENCES

- “Dual Graph Convolutional Network for Hyperspectral Image Classification With Limited Training Samples” by Xin He , Yushi Chen ,and Pedram Ghamisi. (2021)
- A Spectral-Spatial Dependent Global Learning Framework for Insufficient and Imbalance Hyperspectral Image Classification by Qiqi Zhu, Weihuan Deng, Zhuo Zheng, Yanfei Zhong. (2021)
- "HybridSN: Exploring 3D-2D CNN Feature Hierarchy for Hyperspectral Image Classification" by Li et al. (2021)
- “Graph Convolutional Networks for Hyperspectral Image Classification” Danfeng Hong , Member, IEEE, Lianru Gao , Senior Member, IEEE. (2020)
- "FPGA: Fast Patch-Free Global Learning Framework for Fully End-to-End Hyperspectral Image Classification" by Zhang et al. (2021)

Thank You